Supplementary Material on "Quincke rotor dynamics in confinement: rolling and hovering"

Gerardo Pradillo, Hamid Karani and Petia M. Vlahovska

July 12, 2019

1 Numerical simulations

We numerically solve the electrostatic problem within the framework of the leaky dielectric model, i.e. a weakly conducting particle suspended in a poorly conducting liquid. The electric field is irrotational $\mathbf{E} = -\nabla\phi$ and the electric field potential satisfies

$$\nabla^2\phi = 0\,. \tag{1}$$

The computational domain is a rectangle with height $h = 120\,\mu$m and width $w = 3000\,\mu$m. The centroid of the colloid is placed at $w/2$ and its height above the bottom electrode is chosen based on the experimentally measured gap $a + 2.8\mu$m, where a is the colloid radius (In the case of the $a = 20\,\mu$m colloid we use the same gap as we do not have experimental measurements for this particle size). The top and bottom walls are the electrodes and they are treated as equipotential surfaces with the top wall set as ground. The side walls are insulating. The boundary conditions at the colloid surface are the continuity of electric potential and normal component of electric current

$$\phi_{\rm p} = \phi_{\rm m}\,, \quad \sigma_{\rm p}\frac{\partial\phi_{\rm p}}{\partial r} = \sigma_{\rm m}\frac{\partial\phi_{\rm m}}{\partial r} \tag{2}$$

We benefit from the analogy of the governing equations and interface boundary conditions of the Ohmic model (Eqs. (1) and (2)) with those of heat conduction and use ANSYS Fluent package for performing the numerical computations. We obtain the electric field distribution by evaluating the gradient of the electric potential.

2 Dielectrophoretic force

A particle in a nonuniform electric field experiences dielectrophoretic (DEP) force which in DC electric field can be estimated from

$$F_{DEP} = 2\pi a^3 \varepsilon_m \frac{R-1}{R+2} \nabla |E|^2$$

The direction of the DEP force depends on the conductivity ratio $R = \sigma_p/\sigma_m$. If the particle is more polarizable (conducting) than the suspending medium, i.e., $R > 1$, the particle moves in the direction of increasing electric field. This is known as positive dielectrophoresis. In the opposite case, which corresponds to the Quincke configuration, the particle's motion is away from high field regions.

When moisture is introduced via the surfactant, the water can adsorb at the particle surface thereby changing the particle electrical properties [1]. To estimate of the conductivity of the moisture covered particle, we consider a thin shell model: a sphere of radius a coated with a water layer of thickness δ with conductivity σ_w, see Fgure 2

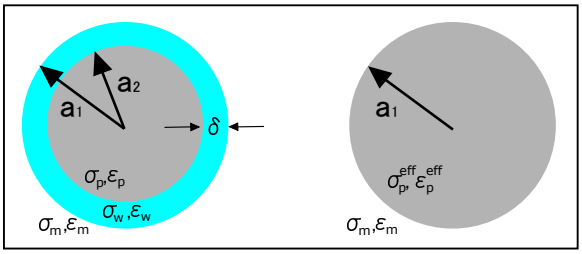

Supp. Fig. 1: a) Particle with an adsorbed moisture layer of thickness δ at the particle interface. b) Equivalent homogeneous particle system.

$$\sigma_p^{eff} = \sigma_w \left[\frac{((a+\delta)/a)^3 + 2(\sigma_p - \sigma_w)/(\sigma_p + 2\sigma_w)}{((a+\delta)/a)^3 - (\sigma_p - \sigma_w)/(\sigma_p + 2\sigma_w)} \right] \tag{3}$$

If $\sigma_p < \sigma_w$ and $\delta << a$,

$$\bar{\sigma}_p^{eff} = \sigma_p + 2\sigma_w \delta/a\,, \tag{4}$$

Here we estimate the thickness of the water layer in our experiments assuming water conductivity $\sigma_w = 10^{-4}$ S/m.

The water introduced in the chamber via the moist AOT may remain absorbed in the bulk fluid and adsorb at any of the solid surfaces present in the system, i.e. particle and electrodes. The water on the particle is

$$m_p^w = m_{surf}^w \left(\frac{A_p}{A_{sub} + A_p} \right) \tag{5}$$

where m_{surf}^w is the amount of water adsorbed on all surfaces. We estimate that at most 2% of the water added with the AOT is bound to the surfaces, i.e., $m_{surf}^w = 0.02 m_w$ with m_w is the water mass in the AOT. A higher proportion would lead to effective particle conductivity sufficiently high to reverse polarization and suppress

the Quincke effect.The shell thickness δ is estimated as

$$\delta = \frac{V_p^w}{A_p} \text{ where } V_p^w = m_p^w/\rho_w \tag{6}$$

Our estimations of shell thickness δ, and effective particle σ_p^{eff}, and fluid σ_m conductivities, for 0.05M, 0.1M and 0.15M AOT concentrations considering all cases where moisture are tabulated in Table 1. The water layer thickness is in good agreement to the values reported in [1]

0.05 mol/L				0.1 mol/L				0.15 mol/L			
m (g)	δ (nm)	σ_p^{eff} (nS/m)	σ_m (nS/m)	m (g)	δ nm (nm)	σ_p^{eff} (nS/m)	σ_m (nS/m)	m (g)	δ nm (nm)	σ_p^{eff} (nS/m)	σ_m (nS/m)
0.0082	0.49	1.97	6.83	0.0129	0.77	3.1	19.92	0.0082	0.49	1.97	22.87
0.0181	1.09	4.34	10.1	0.0165	0.99	3.96	21.29	0.0129	0.77	3.10	25.62
0.0251	1.51	6.02	13	0.0323	1.94	7.75	26.35	0.0204	1.22	4.90	35.74
0.0381	2.29	9.14	30.3	0.0528	3.17	12.67	52.85	0.0398	2.39	9.55	42.83

Supp. Table 1: Moisture layer thickness δ, and effective particle σ_p^{eff} and fluid σ_m^{eff} conductivities for the studied molar concentrations.

Table 1 shows that while the conductivity of the fluid varies little with moisture (see also Table 2 of the main text), even a tiny amount of moisture will considerably rise the effective particle's conductivity from $O(10^{-17})$ to $O(10^{-9})$ S/m, making it comparable to the effective conductivity of the fluid. This reduces the non-uniformity of the field around the particle, see Figures 3 and 4, thereby decreasing the magnitude of the DEP force and hindering levitation.

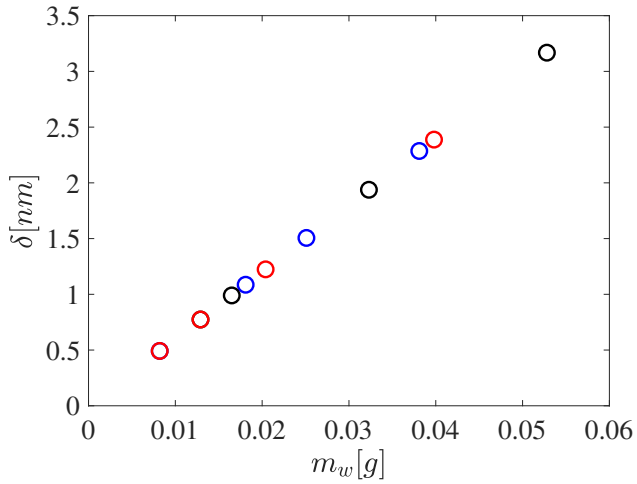

Supp. Fig. 2: Moisture surface layer thickness δ as a function of AOT moisture content $m_w$in grams for 0.05M (Blue), 0.1M (Black) and 0.15M (Red) concentrations. The shell width increases linearly with the moisture absorbed by the AOT.

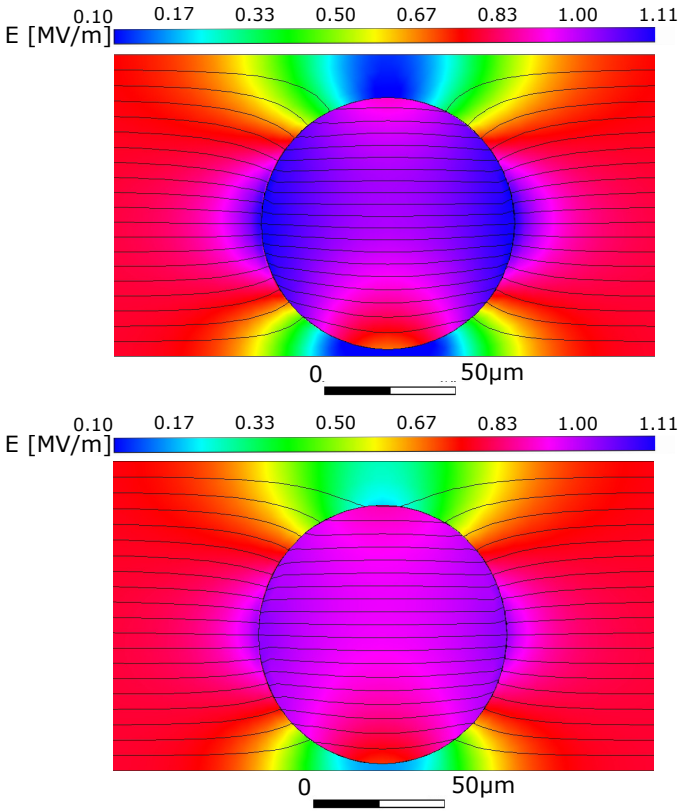

Supp. Fig. 3: top) Dry case: particle with conductivity $\sigma_p = 10^{-17}$ S/m ; bottom) Moisture case: particle with effective conductivity $\sigma_p^{eff} \approx 10^{-9}$ S/m. The suspending medium conductivity is $\sigma_m = 2 \times 10^{-8}$S/m, in d/h = 0.83 confinement. The potential difference is 90V and the particle is suspended at a height of 2.8 μm above the bottom electrode. The electric field is highly distorted in the proximity of the particle and its distribution is clearly asymmetrical in the y-direction.

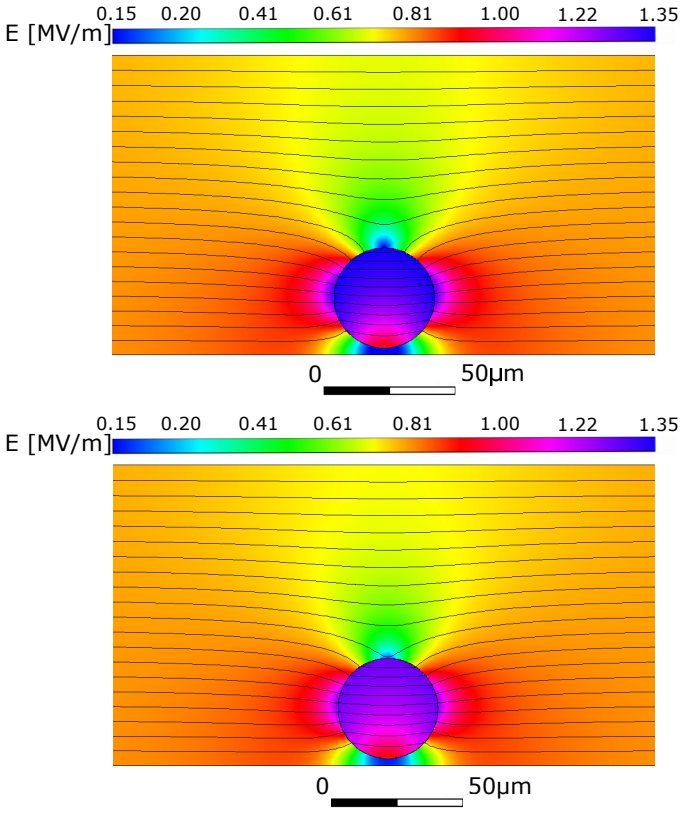

Supp. Fig. 4: top) Dry case: particle with conductivity $\sigma_p \approx 10^{-17}$ S/m ; bottom) Moisture case: effective particle with conductivity $\sigma_p^{eff} \approx 10^{-9}$ S/m; Other conditions same as previous figure.

3 Lift and onset of rotation in the dry AOT system

Figure 5 shows the Lift and Quincke thresholds as a function of the AOT concentration.

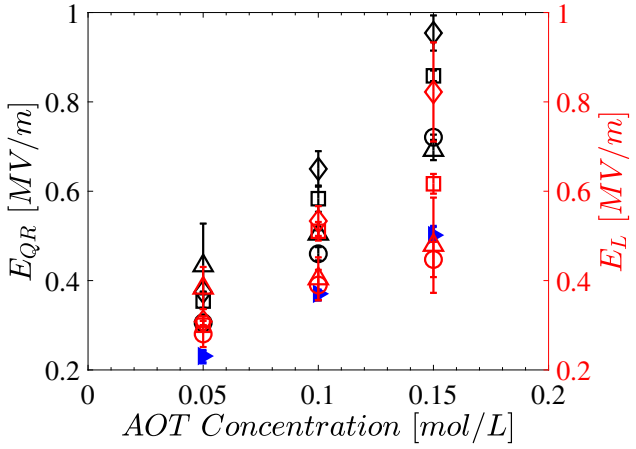

Supp. Fig. 5: Lift and Quincke thresholds, E_L and E_{QR}, of hovering particles for 0.05, 0.1 and 0.15 mol/L solutions of AOT-Hexadecane at zero moisture content for confinements $\diamond : d/h = 0.83$, $\square : d/h = 0.42$, $\triangle : d/h = 0.33$, $\circ : d/h = 0.17$. The rotation thresholds obtained from the theoretical equation for an unbounded domain are shown with blue filled triangles.

	0.05 mol/L		0.1 mol/L		0.15 mol/L	
d/h	E_L (V/m)	E_{QR} (V/m)	E_L (V/m)	E_{QR} (V/m)	E_L (V/m)	E_{QR} (V/m)
0.83	3.08×10^5	3.75×10^5	5.33×10^5	6.50×10^5	8.22×10^5	9.54×10^5
0.42	3.00×10^5	3.54×10^5	5.10×10^5	5.83×10^5	6.17×10^5	8.58×10^5
0.33	3.83×10^5	4.33×10^5	4.04×10^5	5.04×10^5	4.79×10^5	6.92×10^5
0.17	2.81×10^5	3.06×10^5	3.90×10^5	4.60×10^5	4.47×10^5	7.21×10^5

Supp. Table 2: Lift and rotation thresholds for the dry AOT for all confinement conditions.

Figure 6 shows the dependence on confinement of the thresholds for lift and rotation E_L and E_{QH} for the 0.05M and 0.15M AOT system (0.1M is shown in the main text). The general trend is that confinement increases the thresholds, which is expected since larger confinement results in stronger viscous resistance to the sphere rotation. However, in the lowest AOT concentration (0.05M) the dependence is nonmonotonic and shows that lift (and rotation) at $d/h = 0.33$ require stronger field than $d/h = 0.42$. The increase is likely linked to the fact that the particle size is different in these cases - $d/h = 0.33$ corresponds to a particle with diameter 40 μm, while $d/h = 0.42$ corresponds to a particle with diameter 100 μm. In the latter case the dielectrophoretic force is stronger (as it scaled with the cube of the sphere radius) and thus requires lower field strength for lift off. Since the hovering heights in these case would likely to be different, the onset of rotation is also affected. In higher AOT concentrations such nonmonotonic dependence is not observed, likely due to the fact that the conductivity of the fluids is higher and dominates over the particle size in determining the dielectrophoretic force.

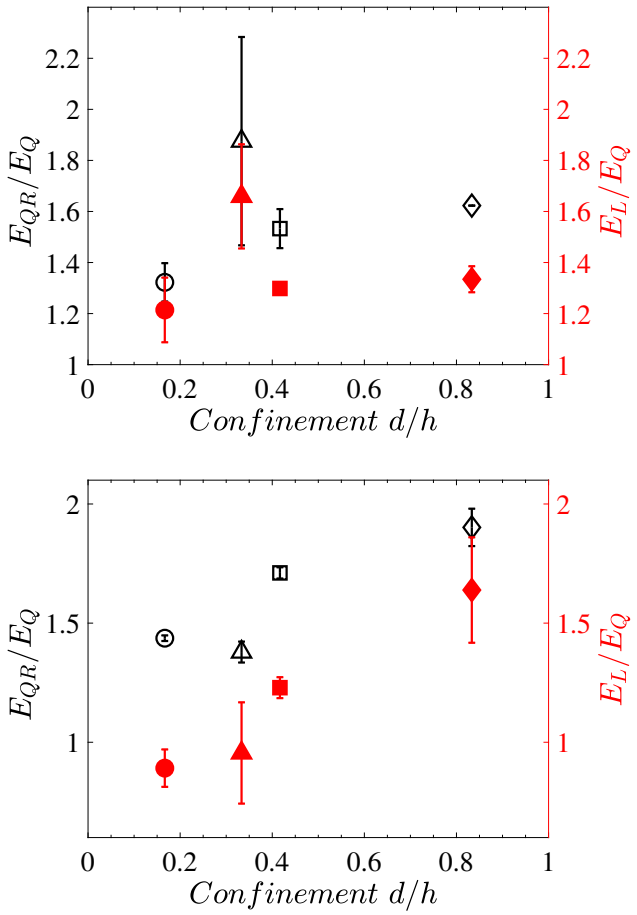

Supp. Fig. 6: Thresholds for lift (right vertical axis) and rotation (left vertical axis) as a function of confinement for a 0.05M (top)and 0.15M (bottom) AOT-Hexadecane solution. The thresholds have been non-dimensionalized by the Quincke threshold calculated from the theoretical equation using the conductivity of the moisture-free fluid of the same AOT concentration.

d/h = 0.83				d/h = 0.42			
0.1 mol/L		0.15 mol/L		0.1 mol/L		0.15 mol/L	
Field (V/m)	Re	Field (V/m)	Re	Field (V/m)	Re	Field (V/m)	Re
1.00×10^6	0.23	1.00×10^6	0.03	1.00×10^6	0.40	1.00×10^6	0.36
1.67×10^6	0.68	1.67×10^6	0.63	1.25×10^6	0.59	1.25×10^6	0.60
3.33×10^6	1.37	3.33×10^6	1.55	1.67×10^6	0.88	1.67×10^6	1.03
5.00×10^6	1.93	5.00×10^6	2.11	2.50×10^6	1.50	2.50×10^6	1.82
6.67×10^6	2.37	6.67×10^6	2.64	3.33×10^6	1.98	3.33×10^6	2.59
8.33×10^6	3.07	8.33×10^6	3.30	4.17×10^6	2.51	4.17×10^6	3.24
-	-	-	-	5.16×10^6	3.33	5.16×10^6	4.11

Supp. Table 3: Field magnitudes and Reynolds number for the hovering rotors at different salt concentrations and confinement conditions (Fig 12 in main text).

4 Onset of rolling at different moisture

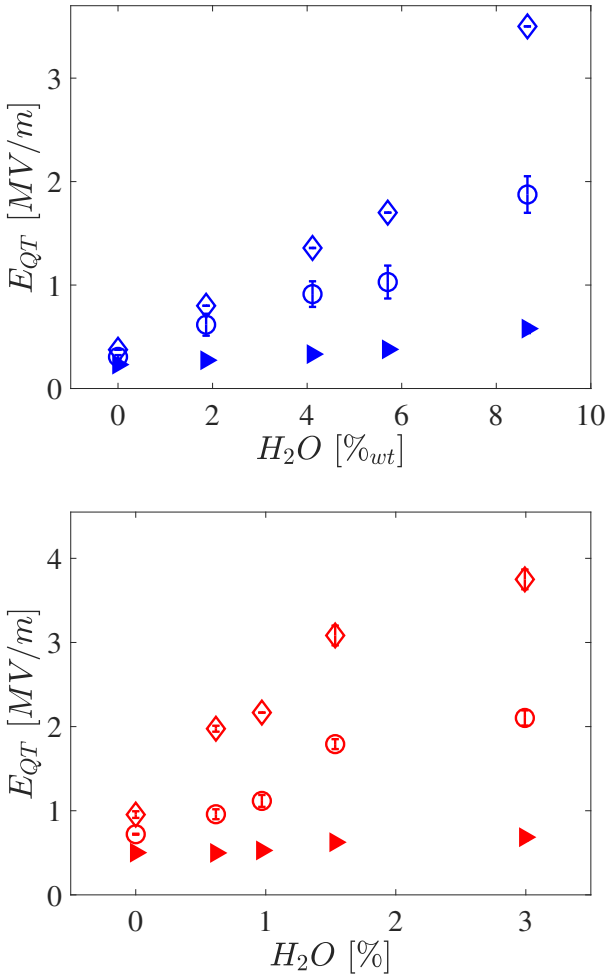

Supp. Fig. 7: Quincke rolling thresholds for 0.05M and 0.15M AOT-Hexadecane solution as a function of moisture content. The symbols correspond to particle confinement $\diamond : d/h = 0.83$, and $\bigcirc : d/h = 0.17$. The filled symbols are the threshold for unconfined electrorotation calculated from the theory for unbounded Quincke rotation using the conductivities for the given AOT and moisture content, Table 2 in the main text. The threshold for Quincke rotation in the hovering state for the dry system ($H_2O\% = 0$) is also shown for comparison.

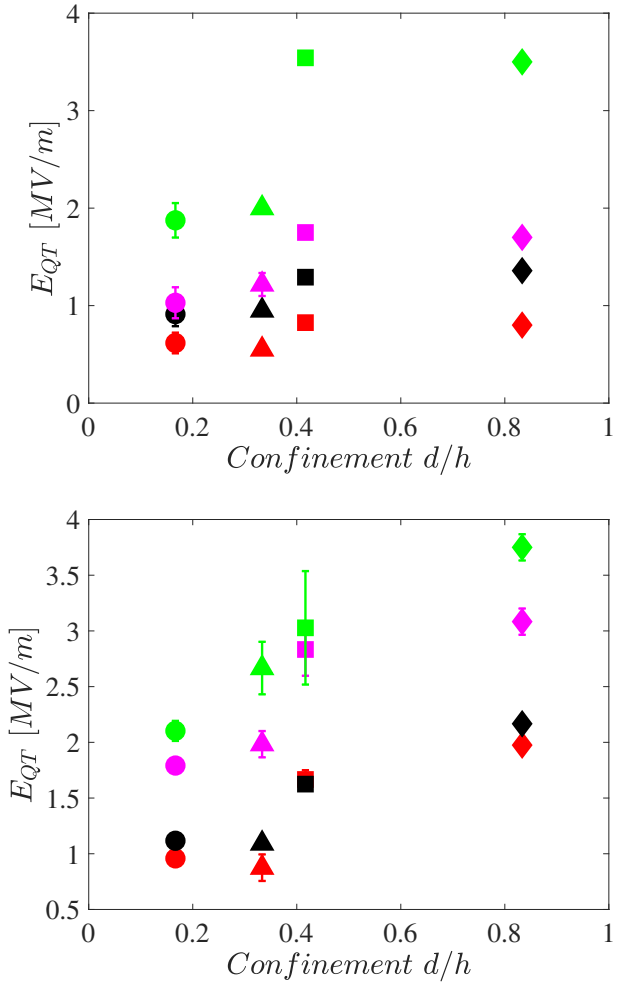

Supp. Fig. 8: Quincke rolling thresholds for 0.05M and 0.15M AOT-Hexadecane solution as a function of moisture content, where $\%wt_{H_2O}$ = red < black < magenta < green . All confinement conditions are tested $\diamond : d/h = 0.83$, $\square : d/h = 0.42$, $\triangle : d/h = 0.33$, $\bigcirc : d/h = 0.17$.

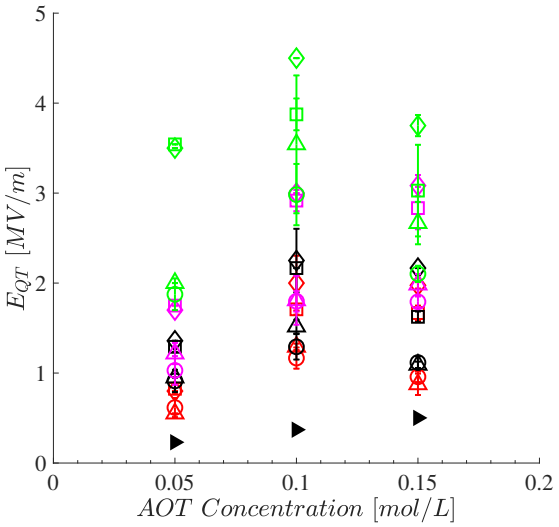

Supp. Fig. 9: Quincke rolling thresholds as a function of AOT concentration and moisture content, where $\%wt_{H_2O}$ = red $<$ black $<$ magenta $<$ green . The confinement conditions are given by, $\diamond : d/h = 0.83$, $\square : d/h = 0.42$, $\triangle : d/h = 0.33$, $\bigcirc : d/h = 0.17$. The plot illustrates the fact that a given salt concentration does not necessarily correspond to a unique threshold value for the onset of rolling E_{QT}. This is due to the moisture in the fluid. The theoretical thresholds calculated using the conductivities for for the moisture free solutions, Table 2 in the main text, are given by the black triangles and lie beneath the experimental values.

5 Lack of Quincke effect in the AOT free hexadecane

The Quincke effect is not observed in pure (AOT-free) hexadecane or at sub- and near- CMC concentrations. Under these conditions the fluid conductivity is very low, see Figure 10, and likely there are insufficient free charges to polarize the sphere.

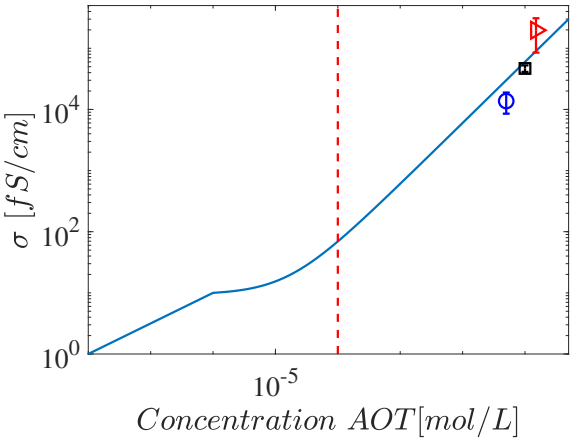

Supp. Fig. 10: Fluid conductivity as function of AOT concentration. The symbols correspond to the AOT concentrations in our experiments. The blue line is obtained from theory [2]. The vertical red line corresponds to the concentration below which Quincke is no longer observed in all of our confinement configurations.

References

[1] T. N. Tombs and T. B. Jones. Effect of moisture on the dielectrophoretic spectra of glass spheres. IEEE Transactions on Industry Applications, 29(2):281–285, March 1993.

[2] Sunil K. Sainis, Jason W. Merrill, and Eric R. Dufresne. Electrostatic Interactions of Colloidal Particles at Vanishing Ionic Strength. Langmuir, 24(23):13334–13347, DEC 2 2008.